Quinolone 3-Carboxylic Acid Pharmacophore: Design of Second Generation HIV-1 Integrase Inhibitors

Raveendra Dayam,[†,§] Laith Q. Al-Mawsawi,[†] Zahrah Zawahir,[†] Myriam Witvrouw,[‡] Zeger Debyser,[‡] and Nouri Neamati*[,†]

Department of Pharmacology and Pharmaceutical Sciences, University of Southern California, School of Pharmacy, 1985 Zonal Avenue, Los Angeles, California 90089, and Molecular Medicine, Katholieke Universiteit Leuven and IRC KULAK, Kapucijnenvoer 33, B-3000 Leuven, Flanders, Belgium

Received May 25, 2007

Two decades of intensive research efforts have led to the discovery of a large number of HIV-1 integrase (IN) inhibitors. Recently, the United States Food and Drug Administration (US FDA) approved MK-0518, or raltegravir (**1**), as the first IN inhibitor for HIV/AIDS treatment. Growing clinical evidence also demonstrates that the emergence of HIV-1 virus strains bearing IN amino acid substitutions that confer resistance to IN inhibitors is inevitable. The discovery of second generation inhibitors with potency against viral strains bearing drug resistant IN substitutions is necessary for ongoing effective treatment of viral infections. We generated common feature pharmacophore hypotheses using a training set of quinolone 3-carboxylic acid IN inhibitors, including the clinical candidate GS-9137 (**2**). A database search of small molecules using the quinolone 3-carboxylic acid pharmacophore model, followed by in vitro evaluation of selected hits in an assay specific to IN, resulted in the discovery of potential leads with diverse structural scaffolds useful for the design of second generation IN inhibitors.

Introduction

The advent of highly active antiretroviral therapy (HAART[a]) regimens comprised of more than 20 US FDA approved antiretroviral drugs transformed the once fatal HIV/AIDS disease into a chronic infection. HAART combination regimens suppressed viral loads to undetectable levels but failed to eradicate the HIV-1 virus from infected patients. Because of the chronic nature of HIV-1 infection, a life long HAART regimen is required for infected patients. Rapidly emerging multidrug resistant HIV-1 virus strains and severe adverse effects from long-term HAART medication necessitate a demand for potent and safe drugs targeting alternative steps in the HIV-1 replication process.[1–10] The recent progress in the discovery and clinical development of HIV-1 integrase (IN) inhibitors and chemokine receptor (CCR5 and CXCR4) antagonists as novel antiretroviral agents stimulates a new hope in the treatment of HIV/AIDS.[11–14]

IN mediated catalytic reactions are essential for the HIV-1 replication process and sustained viral infection.[15,16] IN mediates integration of the viral cDNA into the host genome through two unique catalytic reactions. In the first step, which takes place in the cytoplasm of an infected cell, IN recognizes newly transcribed viral cDNA and selectively cleaves two nucleotides (GT) from its conserved 3′-CAGT ends. This reaction is called 3′-processing and produces nucleophilic hydroxyls on both 3′-ends (3′-CA-OH) of the viral cDNA. IN translocates to the nucleus of the infected cell along with the processed viral cDNA and several cellular cofactors as a part of the preintegration complex. In the second step, which takes place in nucleus of the infected cell, IN mediates the nucleophilic attack of both 3′- end hydroxyls of the viral cDNA onto the host DNA. This insertion (integration) process is called the strand transfer reaction. Specific in vitro assays have been developed for these reactions by using recombinant IN, a 21-mer DNA substrate representing the U5 region of the HIV-1 long terminal repeat (LTR) regions, and metal cofactors, Mg^{2+} or Mn^{2+}. These in vitro assays have been used to discover a plethora of IN inhibitors from diverse chemical classes.[14,17–21]

The discovery of the β-diketoacid class of IN inhibitors was a major advance in the validation of IN as a therapeutically viable antiretroviral drug target.[22] Several first generation IN inhibitors are in various stages of clinical trials. S-1360 (**3**), a β-diketoacid bioisostere, was the first IN inhibitor to enter into human clinical trials (Figure 1).[23] Compound **3** showed potent antiviral activity against a variety of HIV-1 clinical isolates. Consistent with its specificity to IN, **3**-resistant IN mutant proteins have been isolated in vitro. The amino acid substitutions of IN conferring resistance to **3** are T66I, Q148K, I151L, and N155S.[23] Unfortunately, **3** failed to show efficacy in HIV-1 infected patients due to its metabolic instability.[24,25] Currently, GS-9137 (**2**) is in advanced stages of clinical trials (Figure 1). The first US FDA approved IN drug as of October 2007, raltegravir (**1**), showed potent antiviral activity against a broad panel of clinical HIV-1 isolates, including isolates resistant to almost all clinically used antiretroviral drugs. Compound **1** showed excellent therapeutic efficacy in antiretroviral treatment-naive and treatment-experienced HIV-1 infected patients.[26–29] Similar to those of **3**, the IN amino acid substitutions conferring resistance to **1** have emerged under drug pressure. The IN substitutions conferring resistance to **1** were T66I, L74M, E92Q, Y143R/C, Q148K/R/H, and N155H.[28,29] Compound **2**, currently in late-stage clinical trials, belongs to the quinolone 3-carboxylic acid class of IN inhibitors.[30–32] In phase II clinical studies, **2** showed significant antiretroviral activity in antiretroviral treatment-naive and treatment-experienced HIV-infected patients when compared with a placebo. Similar to those of other

* To whom correspondence should be addressed. Phone: 323-442-2341. Fax: 323-442-1390. E-mail: neamati@usc.edu.

† University of Southern California.

‡ Katholieke Universiteit Leuven and IRC KULAK.

§ Current address: Informatics Division, GVK Biosciences Private Limited, Hyderabad, India.

[a] Abbreviations: HIV, human immunodeficiency virus; IN, integrase; HAART, highly active antiretroviral therapy; FDA, Food and Drug Administration; HBA, H-bond acceptor; HRA, hydrophobic aromatic; NI, negative ionizable; IC_{50}, inhibitory concentration at 50%; $CCID_{50}$, cell culture infective dose at 50%.

10.1021/jm070609b CCC: $40.75
Published on Web 02/19/2008

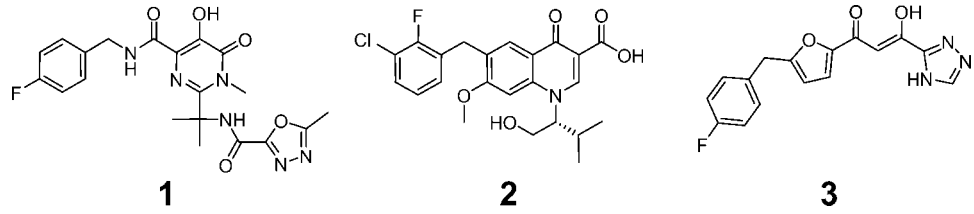

Figure 1. Clinically studied HIV-1 integrase inhibitors. Currently, MK-0518 (**1**) has been US FDA approved, GS-9137 (**2**) is in advanced stage clinical trials, and S-1360 (**3**) failed in clinical trials.

clinically studied inhibitors, amino acid substitutions in the IN catalytic core domain conferring resistance to **2** have been identified. The IN amino acid substitutions conferring resistance to **2** were T66I, E92Q, F212Y, S153Y, and R263K.[33] The dynamic nature of the HIV genome coupled with the requirement of a sustained antiretroviral treatment regimen in chronic HIV-1 patients eventually facilitates the emergence of drug resistant HIV-1 strains. Additionally, previous experiences with other clinically used antiretroviral drugs targeting alternative stages in the HIV-1 life cycle forecast an inevitable emergence of HIV-1 virus strains bearing drug resistant amino acid substitutions in IN once first generation IN inhibitors are commonly used in the clinic. This indicates an obvious demand for the discovery of highly potent second generation IN inhibitors to stay ahead of rapidly emerging drug resistant HIV-1 strains. Here we report the generation and successful use of pharmacophore models based on key chemical features of a set of **2** analogues in the discovery of novel and structurally diverse IN inhibitors.

Results and Discussion

Quinolone 3-Carboxylic Acid Pharmacophore. Quinolone 3-carboxylic acids are a novel class of IN inhibitors.[30] Researchers at Japan Tobacco discovered this class of IN inhibitors through modification of antibiotic quinolones. The quinolone 3-carboxylic acids **4**–**7** and **2** inhibited the strand transfer activity of IN with IC_{50} values ranging from 43.5 ± 8.8 to 7.2 ± 2.2 nM (Table 1). They also inhibited HIV-1 replication with EC_{50} values ranging from 805 to 0.9 nM, consistent with their inhibitory effect on IN strand transfer activity. A thorough analysis of structural features of the quinolone 3-carboxylic acid IN inhibitors indicates the presence of several pharmacophoric features viz. a negatively ionizable feature representing the quinolone 3-carboxylate group, an H-bond acceptor feature representing the β-ketone, two hydrophobic aromatic features representing the two aromatic rings (6-benzyl and the quinolone core), an H-bond donor feature representing the NH of the quinolone ring (in compound **4**) or a hydroxyl group from substitution on N1 of the quinolone ring in compounds **5**–**7** and **2**, and an aliphatic hydrophobic feature representing an isopropyl group of substitution on N1 of quinolone ring in compounds **7** and **2**. Structure–activity relationship analysis shows that variation in substitution on N1 of the quinolone ring has marginal influence on the IN inhibition, particularly from compounds **6**–**7** and **2**. Interestingly, the variation is strongly correlated with the antiretroviral potency of the compounds. The marginal effect of substitution on N1 of the quinolone core on inhibition of the IN catalytic activity indicates that this part of the molecule may not be engaged in strong interactions with IN. Intriguingly, the substitution pattern on N1 of the quinolone core significantly contributed to favorable physicochemical properties of the compounds, which led to a dramatic improvement in antiretroviral activity of the compounds. On the basis of these observations, we restricted contributions from the substitution on N1 of the quinolone core to pharmacophore hypothesis by not choosing the H-bond donor and aliphatic hydrophobic features in the pharmacophore modeling process. This pharmacophore hypothesis is expected to characterize a three-dimensional arrangement for pharmacophoric features required to be in a compound to exert the inhibitory effect on the IN catalytic activity. The HIPHOP algorithm within the Catalyst software package (Accelrys, Inc.) was used to generate common feature pharmacophore hypotheses. The HIPHOP algorithm is routinely employed to generate qualitative common feature pharmacophore hypotheses by using a series of active analogue compounds. In principle, the training set compounds considered for common feature pharmacophore modeling are expected to bind to a drug binding site with a similar binding orientation and exert a set of similar interactions in the drug binding site.

A training set consisting of five quinolone 3-carboxylate IN inhibitors was provided to HIPHOP for the generation of the common feature pharmacophore models (compounds **4**–**7** and **2**, Table 1). Pharmacophore features viz. a negatively ionizable feature, an H-bond acceptor feature, and a hydrophobic aromatic feature, which represent the chemical nature of the quinolone 3-carboxylic acid IN inhibitors, are considered in the pharmacophore modeling process. HIPHOP generated 10 common feature pharmacophore hypotheses. Interestingly, all 10 common

Table 1. Structures of the Training Set Quinolone 3-Carboxylic Acid (**4**−**7** and **2**) HIV-1 Integrase Inhibitors Used to Generate Common Feature Pharmacophore Models

Compound[a]	Structure	Strand transfer (IC_{50}, nM)	Antiviral activity (EC_{50}, nM)
4	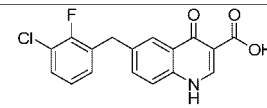	43.5 ± 8.8	805
5	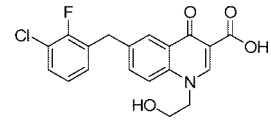	24.2 ± 11.6	76
6	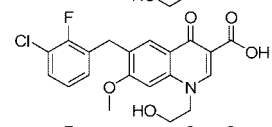	9.1 ± 2.1	17
7	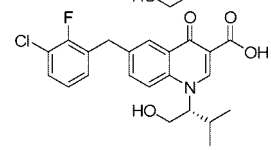	8.2 ± 1.7	7
2	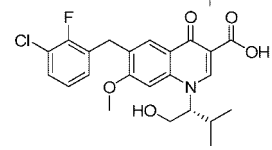	7.2 ± 2.2	0.9

[a] Reference 30.

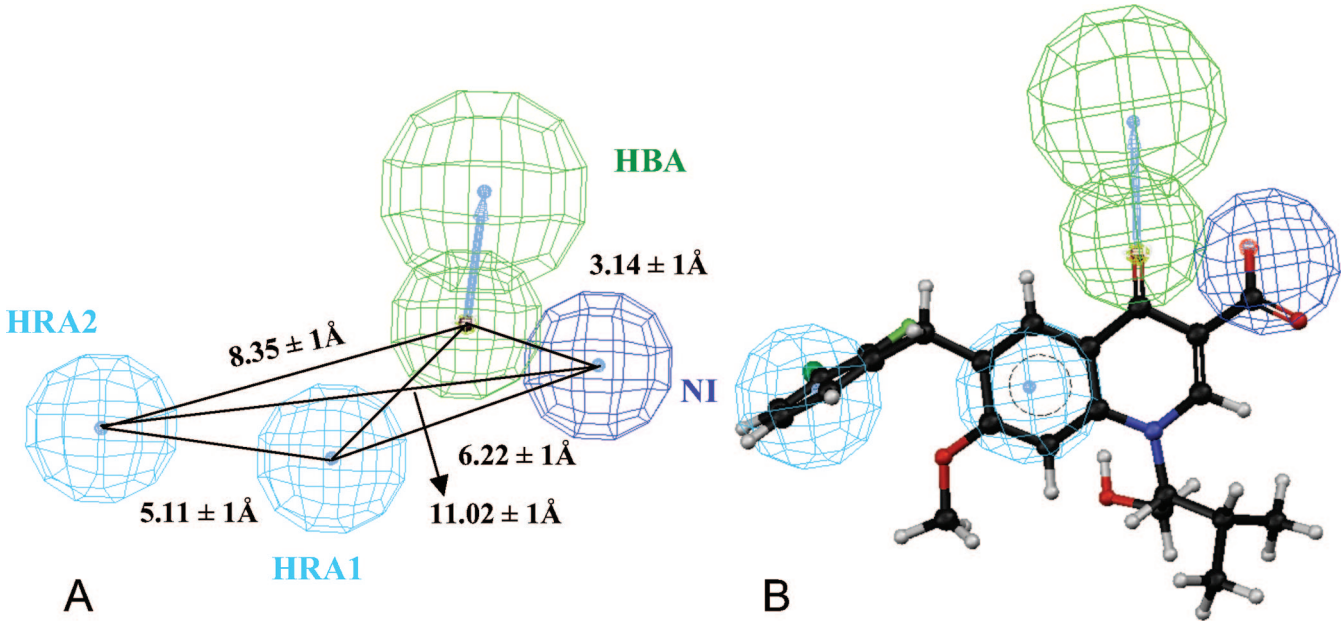

Figure 2. (A) 3D arrangement of the four pharmacophoric features in the quinolone 3-carboxylic acid-based common feature hypothesis 1 (Hypo 1). (B) The clinically studied HIV-1 integrase inhibitor (**2**) is mapped onto Hypo 1. The pharmacophore features are color coded as follows: H-bond acceptor (HBA) as green, negatively ionizable feature (NI) as blue, and hydrophobic aromatic features (HRA1–2) as cyan. Interfeature distances are given in angstroms.

feature pharmacophore models are comprised of four features viz. a negatively ionizable (NI) feature, an H-bond acceptor (HBA) feature, and two hydrophobic aromatic (HRA) features. However, a careful visual analysis reveals that the direction of the HBA feature with respect to the NI feature varies in all 10 common feature pharmacophore models. The orientation of the remaining two HRA features with respect to the NI feature is almost similar in all 10 models. HIPHOP ranked all returned pharmacophore hypotheses based on how well a hypothesis is mapped onto the key chemical features of all five training set compounds. Similar to the β-diketo acid class of IN inhibitors, **2** and its analogues are believed to interact with the active site Mg^{2+} ions and thereby disrupt IN catalytic activities. The carboxylate and β-ketone groups of the quinolone 3-carboxylic acid IN inhibitors are proposed to be involved in chelation of the active site Mg^{2+} ions. The orientation of HBA and NI features in pharmacophore hypothesis one (one of the 10 hypotheses generated by HIPHOP) is in accord with the proposed binding mechanism of the quinolone 3-carboxylate IN inhibitors. We considered pharmacophore hypothesis one (Hypo1) as a representative quinolone 3-carboxylic acid pharmacophore, based on the relative orientation of the HBA and NI features (Figure 2A). HIPHOP also ranked Hypo1 as the best pharmacophore hypothesis among the 10 returned pharmacophore hypotheses. The inter feature distance between optimally oriented HBA and NI features in Hypo 1 is 3.14 ± 1 Å (Figure 2A). The distances between the key NI feature and the two hydrophobic aromatic features (HRA1 and 2) in Hypo 1 are 6.22 ± 1 and 11.02 ± 1 Å, respectively. The inter feature distances between HBA and the HRA1 and 2 in Hypo1 are 4.26 ± 1 and 8.35 ± 1 Å, respectively. HRA1 and HRA2 are separated by a distance of 5.11 Å. Mapping of Hypo 1 onto the clinically studied **2** shows an excellent agreement (3.95/4.0) between key chemical features of the compound and the pharmacophoric features of Hypo 1 (Figure 2B). In addition, Hypo 1 successfully retrieved a large number of known IN inhibitors from an in-house small-molecule database (data not shown). On the basis of a sensible arrangement of its key pharmacophoric features and its ability to distinguish known IN inhibitors, we selected Hypo 1 to utilize as a search query to retrieve novel compounds with optimum arrangement of pharmacophoric features and diverse structural scaffolds from a database of commercially available small-molecules.

Compound Selection. Hypo 1 retrieved 1978 compounds from a database of 362 260 commercially available small-molecules. A compound could be retrieved as a hit only when all features of the pharmacophore were mapped by the chemical features of the compound. A smaller number of hits, 0.54% of the target database, indicates distinctiveness of the Hypo1 in retrieving compounds. The pharmacophore fit value was calculated for all of the hits using Hypo1. Two hundred compounds out of 1978 hits mapped onto Hypo 1 with a fit value ≥ 1.50 and were selected for further analysis. Visual examination of the mapping of all 200 compounds onto Hypo1 was performed to ensure pharmacophoric features are reasonably mapped onto chemical features of the compounds. In particular, the orientation of the NI and HBA features in the same plane was monitored for each compound after mapping of the Hypo1 onto the compounds. In addition, all compounds with interesting chemical and structural features were docked onto the IN active site to predict their possible binding orientation and the specific interactions with active site amino acid residues. Predicted binding orientations and possible interactions exerted by the compounds inside the IN active site were visually examined. Finally, we selected 56 hits to evaluate for IN inhibitory activity using an in vitro assay. The primary selection was performed based on the pharmacophore fit value of the compounds and on the relative orientation of key chemical features of compounds when mapped by Hypo1. We also considered the predicted binding orientation of the compounds inside the IN active site and the key interactions exerted by the compounds with prominent amino acid residues in the IN active site as an additional selection criterion.

Inhibition of HIV-1 Integrase Catalytic Activities by Pharmacophore Hits. The selected 56 pharmacophore hit compounds were purchased from a commercial chemical

Table 2. HIV-1 Integrase Inhibitory Activities of Novel Compounds Retrieved by Pharmacophore Model 1 from a Database of 360 000 Small-Molecule Compounds

Compound	Structure	3′-Processing (IC_{50}, μM)	Strand transfer (IC_{50}, μM)	Pharmacophore Fit Value
8	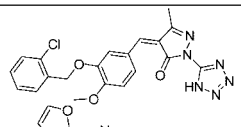	14 ± 7	5 ± 3	3.1
9	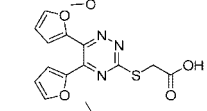	18 ± 4	5 ± 3	2.3
10	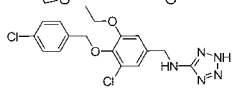	>100	52 ± 8	1.7
11	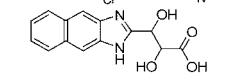	>100	46 ± 12	2.9
12	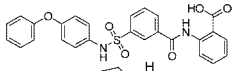	42 ± 10	18 ± 3	3.5
13	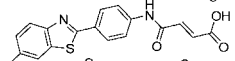	48 ± 19	23 ± 4	3.1
14	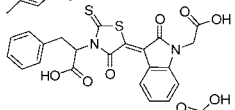	92 ± 17	66 ± 17	3
15	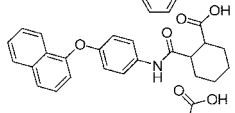	>100	34 ± 7	3.8
16	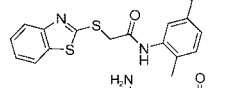	63 ± 22	17 ± 2	1.53
17	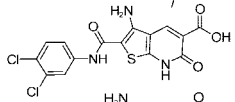	14 ± 6	5 ± 4	1.7
18	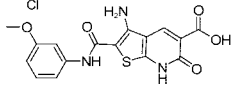	82 + 13	43 + 12	1.7

supplier. Chemical structures and the purity of the compounds were confirmed before initiation of the biological assay. Compounds were screened in an in vitro enzymatic assay specific to IN by using a previously reported method. Of the 56 tested, 11 compounds inhibited the IN catalytic activities with an IC_{50} value < 100 μM. Five out of 11 active compounds inhibited the strand transfer activity of IN with an IC_{50} value < 20 μM. The relatively high rate (19.6%) in the discovery of active hits demonstrates the proficiency and advantage of active-analogue based pharmacophore modeling in the identification of leads with diverse structural scaffolds to enrich a strong pipeline of potent therapeutics targeting a pathogen as genetically dynamic as HIV-1. The chemical structures, the IN inhibitory activities, and the pharmacophore fit values of the active compounds are given in Table 2. Mapping of compound **8** onto Hypo1 shows a good agreement (3.1/4.0) between chemical features of the compound and pharmacophoric features of Hypo 1 (Figure 3A). Compound **8** inhibits both 3′-processing and strand transfer activities of IN with IC_{50} values of 14 ± 7 and 5 ± 3 μM, respectively. The dose dependent inhibitory effects displayed by compound **8** on the 3′-processing and strand transfer activities of IN are shown in a gel image along with other active compounds **9**, **12**, **14**, and **18** in Figure 4. The mapping pattern of the NI, HBA, and HRA1 features onto the tetrazole (a bioisostere of carboxylic acid), pyrazolone, and benzylidene groups of compound **8** is very similar to the mapping of the features onto the training set quinolone 3-carboxylic acids (Figure 2B). A high probability of the tetrazole and benzylidene-pyrazolone groups of compound **8** to maintain a planar orientation and to adopt a conformation favorable to chelate the active site Mg^{2+} further supports the observed IN inhibitory activity of the compound. Considering the novel structural features and interesting dose dependent IN inhibitory profile of compound **8**, we designed a structure–activity relationship study around the core of the compound. We defined a minimum substructure (substructure A) important for the IN inhibitory activity of compound **8** to search a database of commercially available small-molecules (Figure 5A). A search using substructure A as a query retrieved five analogues of compound **8** (Table 3). Similar to compound **8**, its analogues **19**−**23** showed a very strong inhibitory profile against both the 3′-processing and strand transfer reactions of IN, indicating a coherent structure–activity relationship in this small set of compounds (Table 3). Intriguingly, compounds **19**–**23** could be partially (3 out of 4 features) mapped by pharmacophoric features of Hypo 1. Compounds **19**–**23** showed pharmacophore fit values ranging from 2.30 to 2.44 when a feature of the Hypo 1 is allowed to be missed in the mapping process. The HRA2 feature of Hypo 1 is missing in compounds **19**–**23**. It appears that the structural unit comprised of the tetrazole, pyrazolone, and benzylidene groups of compound **8** that are mapped by key NI, HBA, and HRA1 features of Hypo1 is the minimum required scaffold in this series of compounds for inhibition of the IN catalytic activities. The IN inhibitory profile of compound **8** and its analogues demonstrates that the substitution pattern on the benzylidene group is likely to tolerate significant structural changes. On the other hand, this part of the compound accommodates dramatic structural changes required for optimization of the IN inhibitory activities and physicochemical properties of compound **8** and its analogues. Additionally, we docked compound **8** onto the IN active site to predict its bound conformation. Compound **8** adopted an interesting bound conformation inside the IN active site (Figure 6A). There is a good correlation observed between pharmacophore features (Hypo1) and predicted binding interactions of compound **8** inside the IN active site. For a comparison the bound conformation of 5-CITEP (**24**) from the cocrystal structure of the core domain of IN in complex with **24** is shown in Figure 6B. The predicted bound conformation of compound **8** is different from that of **24** inside the IN active site. The tetrazole and pyrazolone groups of compound **8** interact with the active site Mg^{2+}, which is in accord with pharmacophore mapping. However, the carbonyl oxygen, instead of pyrazolone nitrogen interacts with the Mg^{2+}. The benzylidene and its benzyloxy substituent occupied a wide cavity in the IN active site. The bound orientation of the benzylidene ring explains observed tolerance to substitutions on its *ortho* and *meta* positions. However, large substitutions on the *para* position (**23**) of the benzylidene ring may cause unfavorable steric interactions. Optimized substitution on the benzylidene ring of compound **8** would warrant novel compounds with enhanced IN inhibitory activity as well as favorable physicochemical properties.

Compound **9** with a reasonable pharmacophore fit value (2.3/4.0) inhibited both 3′-processing and strand transfer activities of IN with IC_{50} values of 18 ± 4 and 5 ± 3 μM, respectively (Table 2). Mapping of Hypo 1 onto compound **9** shows a reasonable agreement between the pharmacophore features of Hypo1 and the chemical features of the compound (Figure 3B). Considering its novel structure, we decided to extend screening of analogues of compound **9**. A search using substructure B (Figure 5B) found no analogous compounds in the commercial database of small-molecules. However, a search using substruc-

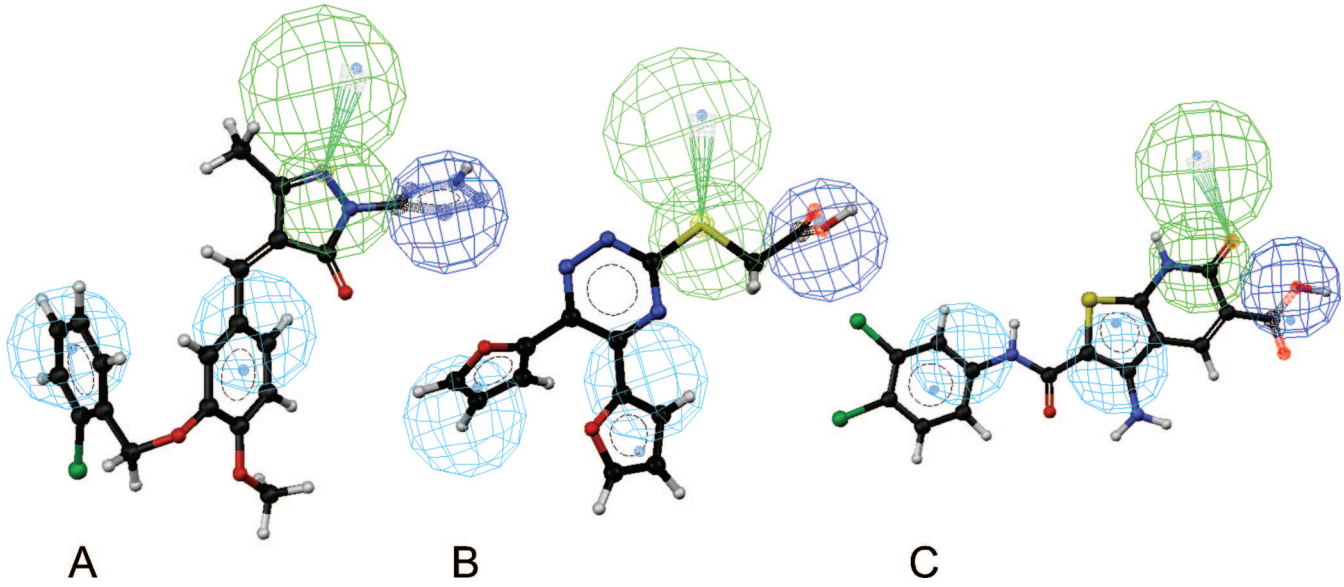

Figure 3. Mapping of the quinolone 3-carboxylic acid-based common feature hypothesis 1 (Hypo 1) onto compounds **8** (A), **9** (B), and **17** (C), which exhibited potent HIV-1 integrase inhibitory activity. A clear agreement between pharmacophoric features of Hypo1 and the chemical features of the active compounds is observed.

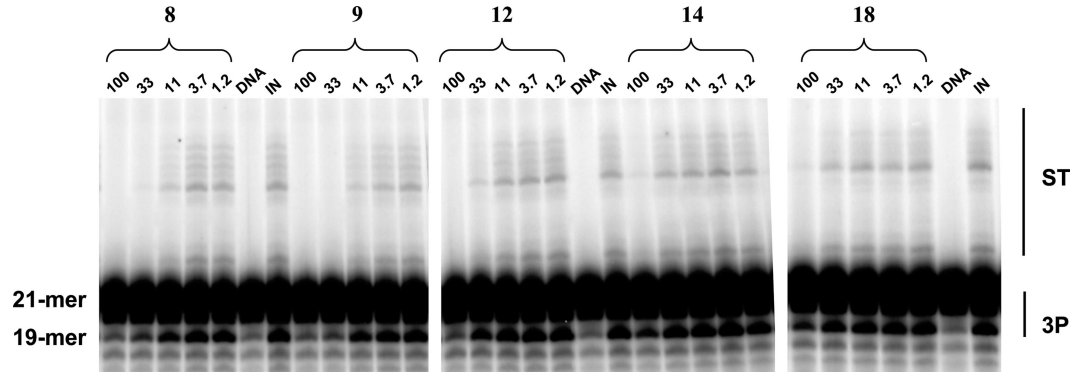

Figure 4. HIV-1 integrase inhibition profiles of some of the active compounds identified using the quinolone 3-carboxylic acid pharmacophore model (Hypo1). Concentrations of each inhibitor are given in micromolar.

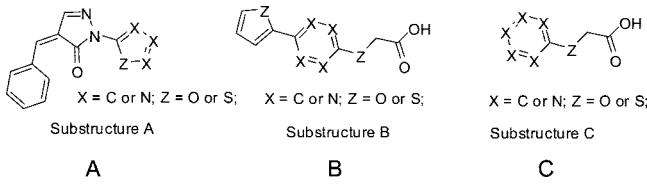

Figure 5. Substructures A−C were used as 2D search queries to retrieve structural analogues of active compounds **8** and **9** from a database of commercially available small-molecules.

ture C (Figure 5C), a pruned substructure B, retrieved a large number of compounds with varied similarity to compound **9**. We selected compounds **25**−**28** to screen in the IN assay (Table 4). Interestingly, with the exception of compound **25**, none of the compounds (**26**–**28**) inhibited the IN catalytic activities at a maximum tested concentration of 100 μM. Compounds **26**–**28** could not be mapped by Hypo 1. Compound **25**, with a slightly improved pharmacophore fit value when compared to compound **9**, exhibited a weak inhibitory activity against both 3′-processing (98 ± 10 μM) and strand transfer (60 ± 12 μM) reactions of IN. Further, it would be interesting to screen close analogues to draw a structure–activity relationship around the core of compound **9**.

Compounds **10** and **11** selectively inhibited the strand transfer activity of IN with IC_{50} values of 52 ± 8 and 46 ± 12 μM, respectively. We also tested several analogues of compound **10** (See Supporting Information, Table S1, **29**–**37**). All of the analogues of compound **10** did not inhibit the IN catalytic activities at a maximum tested concentration of 100 μM. Compounds **12** and **13**, with relatively high pharmacophore fit values of 3.5 and 3.1, respectively, showed ∼2-fold selectivity for inhibition of the strand transfer activity of IN. Compounds **12** and **13** inhibited strand transfer activity of IN with IC_{50} values of 18 ± 3 and 23 ± 4 μM, respectively. These compounds inhibited the 3′-processing activity of IN with IC_{50} values of 42 ± 10 and 48 ± 19 μM, respectively. Compound **14**, with a pharmacophore fit value of 3.0, showed weak inhibitory activities against both the 3′-processing and strand transfer reactions of IN. Compound **14** inhibited 3′-processing and strand transfer activities of IN with IC_{50} values of 92 ± 17 and 66 ± 17 μM, respectively. Besides the required features to inhibit the IN catalytic activities, compound **14** possessed several hydrophilic functional groups, which may have contributed unfavorable interactions toward binding of the compound to IN active site.

Compound **15**, with a high pharmacophore fit value (3.5/4.0), selectively inhibited the strand transfer activity of IN with an

Table 3. HIV-1 Integrase Inhibitory Activity of Compound **8** Analogues

Compound	Structure	3′-Processing (IC_{50}, μM)	Strand transfer (IC_{50}, μM)	Pharmacophore Fit Value
8	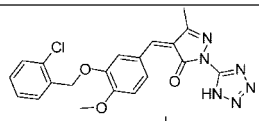	14 ± 7	5 ± 3	3.1
19	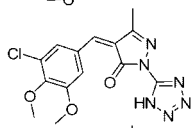	5 ± 2	4 ± 2	(2.31)[a]
20	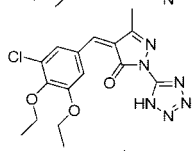	7 ± 6	4 ± 2	(2.44)
21	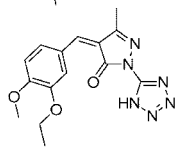	75 ± 28	59 ± 13	(2.31)
22	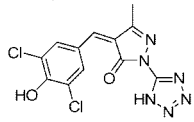	11 ± 3	13 ± 11	(2.30)
23	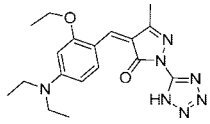	61 ± 8	65 ± 8	(2.30)

[a] Compounds **19**–**23** are partially (3/4 features) mapped by Hypo 1. The pharmacophore fit values are calculated by using a feature missing option.

IC_{50} value of 34 ± 7 μM. The required planarity may not be attained by the structural unit of compound **15**, which was mapped by key NI and HBA features due to the conformational flexibility. Partial oxidation or aromatization of the cyclohexane ring is expected to improve IN inhibitory potential of compound **15**. Compound **16**, with a low pharmacophore fit value, inhibited the 3′-processing and strand transfer activities of IN with IC_{50} values of 63 ± 22 and 17 ± 2 μM, respectively. Interestingly, compounds **12** and **16**, which share a similar chemical arrangement in some part of the compounds (2-acetamidobenzoic acid in **12** and 3-acetamidobenzoic acid in **16**) and were each mapped by the NI and HBA features of Hypo 1, also showed a similar IN inhibitory activity profile. However, the slight variation in the position of the carboxylic acid group in the acetamidobenzoic acid portion of compounds **12** and **16** led to observed differences in pharmacophore fit values.

Compound **17**, with a low pharmacophore fit value, showed strong IN inhibitory activities. The mapping of Hypo 1 onto compound **17** demonstrates a sensible fit between chemical features of the compound and the pharmacophoric features of Hypo 1 (Figure 3C). The arrangement of functional groups on compound **17**, which are mapped by the key pharmacophoric features NI, HBA, and HRA 1 of Hypo 1, supports the possible involvement of these functional groups in the chelation of Mg^{2+} inside the IN active site. However, limited conformational flexibility of compound **17** due to the amide linker between two aryl groups bearing key pharmacophore features contributes to a decreased pharmacophore fit value. Compound **17** inhibited both the 3′-processing and strand transfer activities of IN with IC_{50} values of 14 ± 6 and 5 ± 4 μM, respectively. Surprisingly, compound **18**, a close analogue of compound **17**, showed weak inhibitory activities against both 3′-processing and strand transfer reactions of IN (Table 3). Furthermore, the testing of additional analogues of compound **17** would help to draw a structure–activity relationship model. Also, optimization of key structural features of compound **17**, to further improve its mapping onto the Hypo 1 model, is expected to enhance the IN inhibitory activity of the compound.

We observed a weak correlation between the pharmacophore fit value and the IN inhibitory potency of the active hits. The IN inhibitory profile of the active hits indicates that a high pharmacophore fit value alone does not entirely represent the prerequisites of a compound to establish a set of favorable binding interactions with its target. Overall structure and ability of various functional groups (pharmacophoric features) in a compound to positively contribute to the binding process beyond certain structural constrains also largely determine the activity profile of the compound. To this extent we tried to incorporate these factors in the compound selection process to identify novel IN inhibitors.

Cytotoxicity and Antiviral Results. A positive aspect of using pharmacophoric technologies in drug design programs is the ability to identify numerous potential lead compounds with diverse structural scaffolds that exhibit a desired biological activity. The identified compounds are expected to display diverse pharmacokinetic/pharmacodynamic properties in vivo, providing a range of options when deciding which candidate compounds will be selected for further development. In efforts to determine which IN inhibitory compound classes identified here to select for further development, we evaluated the cytotoxicity of each new IN inhibitor in the NIH3T3 mouse embryonic fibroblast cell line. We additionally evaluated the toxicity and tested 10 representative compounds for antiviral activity against HIV-1 in the human T-cell line MT-4. A few of the inhibitors displayed moderate toxicity in the NIH3T3 mouse embryonic fibroblast cell line at a maximum tested concentration of 10 μM (data not shown). The compounds chosen for cytotoxicity and antiviral activity testing in the HIV relevant human T-cell line MT-4 included **10**–**16**, **19**, **21**, and **26**. In this cell line, none of the compounds, with the exception of compound **15** with a CC_{50} of 3.5 μM, displayed any significant cytotoxicity below 40 μM. Unfortunately, none of the compounds displayed substantial antiviral activity. Optimization efforts are underway to enhance the antiviral activity of our most potent second generation IN inhibitors.

Conclusions

We have developed a four feature quinolone 3-carboxylic acid pharmacophore model using a training set consisting of clinical candidate **2** analogues. We have successfully utilized the quinolone 3-carboxylic acid pharmacophore in the discovery of novel IN inhibitors with diverse structural scaffolds. Further optimization of the active compounds with amenable structural features would provide second generation IN inhibitors with enhanced potency against HIV-1 strains resistant to first generation IN inhibitors.

Methods

Generation of Quinolone 3-Carboxylic Acid Pharmacophore Hypotheses. Common feature pharmacophore hypotheses were generated using a set of five quinolone 3-carboxylic acid IN inhibitors (**4**–**7** and **2**, Table 1). The structures and conformations of the five compounds in their carboxylate form were built within Catalyst (Accelrys, Inc.).[34] The Poling algorithm implemented within Catalyst was used to generate conformations for all of the compounds.[35–37] For each compound, possible diverse sets of conformations were generated over a 20 kcal/mol range using the BEST flexible conformation generation option available in Catalyst.

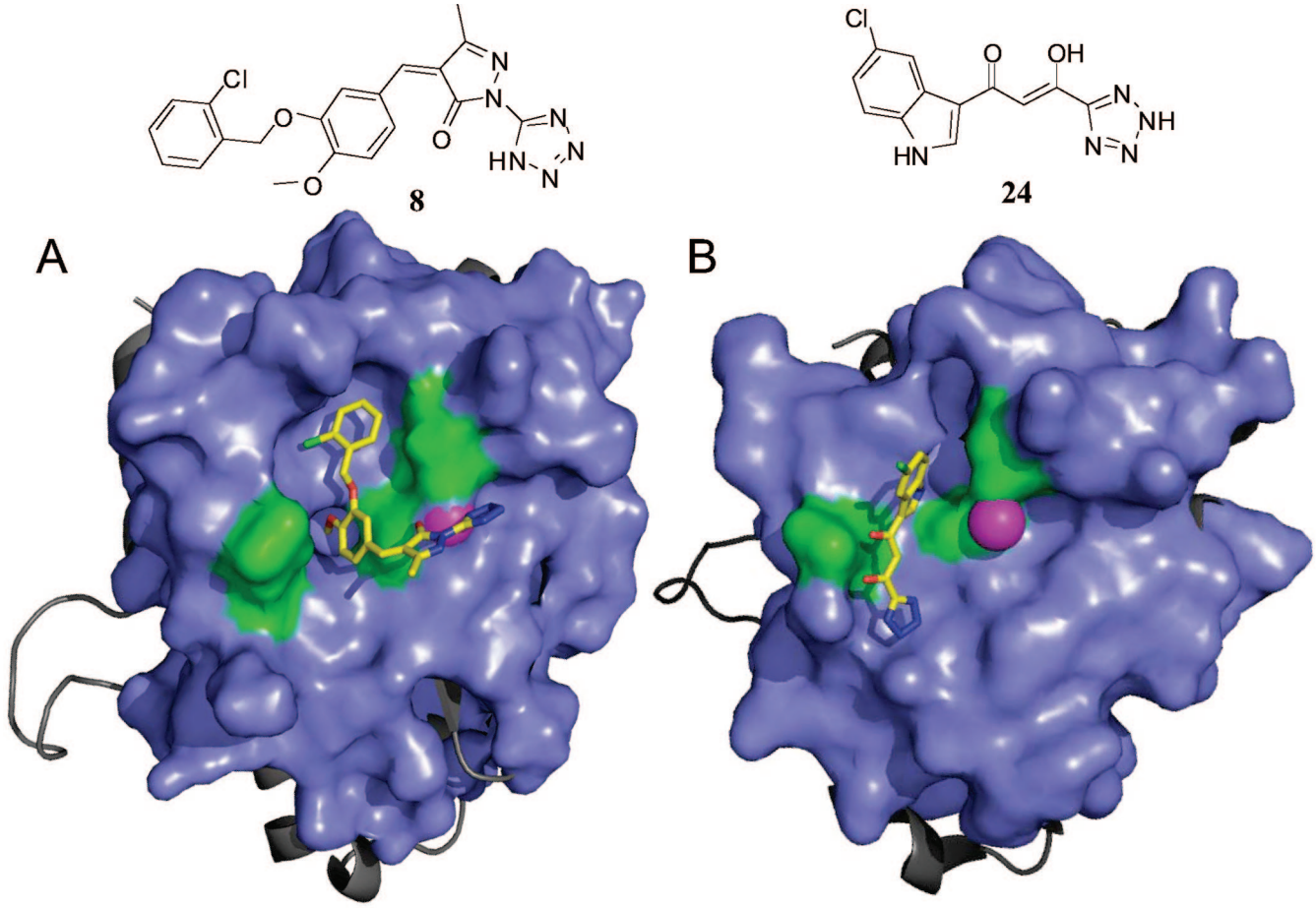

Figure 6. (A) Predicted binding orientation of compound **8** inside the HIV-1 integrase active site. The stick model represents the bound conformation of compound **8**. (B) The bound conformation of 5-CITEP (**24**) extracted from the cocrystal structure of the core domain of HIV-1 integrase and the **24** complex (PDB1QS4). The magenta sphere represents the active site Mg^{2+}, the blue surface represents the active site region of HIV-1 integrase, and the green surface indicates the position of catalytically important residues D64, D116, and E152.

The HIPHOP module in Catalyst was used to generate the common feature hypotheses. HIPHOP evaluates a collection of conformational models of molecules and a selection of chemical features, and it identifies configurations of features (pharmacophore) common to these molecules. The top-ranking pharmacophores are expected to identify the hypothetical orientation of the active compounds and the common binding features interacting with the target. On the basis of the chemical features of the training set quinolone 3-carboxylate IN inhibitors, a set of features were selected to be present in the pharmacophore generation experiment. The chemical features considered in the pharmacophore model generation run were negatively ionizable (NI), H-bond acceptor (HBA), and hydrophobic aromatic (HRA) features. HIPHOP was set to consider these features in the generation of the pharmacophore hypotheses.

Database Search. The representative quinolone 3-carboxylic acid pharmacophore hypothesis (Hypo 1) was used as a search query to retrieve compounds with novel structural scaffolds and desired chemical features from a multiconformer Catalyst-formatted database consisting of 362 260 commercially available compounds (ASINEX Corp, North Carolina, USA). The Fast Flexible Search Databases/Spread Sheets method in Catalyst was used to search the database.

Docking. The subunit B of the core domain X-ray structure of IN (PDB 1BIS), in which all the active site amino acid residues were resolved, was chosen for our docking studies.[38] A Mg^{2+} ion was placed in the active site between carboxylate oxygen atoms of amino acid residues D64 and D116 considering the geometry of the Mg^{2+} ion that was present in the subunit A of IN in PDB 1BIS and subunit A in IN-5CITEP (**24**) complex X-ray structure (PDB 1QS4).[39] All of the water molecules present in the protein were removed, and proper protonation states were assigned for acidic and basic residues of the protein. Docking was performed using version 3.1 of the Genetic Optimization for Ligand Docking (GOLD) software package.[40] GOLD is an automated ligand docking

Table 4. HIV-1 Integrase Inhibitory Activity of Compound **9** Analogues

Compound	Structure	3'-Processing (IC_{50}, μM)	Strand transfer (IC_{50}, μM)	Pharmacophore Fit Value
9	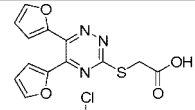	18 ± 4	5 ± 3	2.3
25	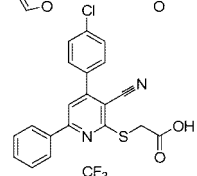	98 ± 10	60 ± 12	2.9
[a]**26**	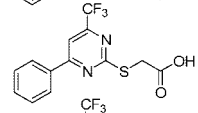	>100	>100	
27	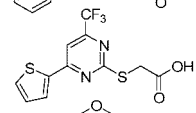	>100	>100	
28	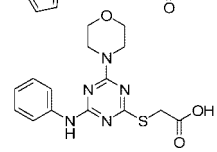	>100	>100	

[a] Compounds **26**−**28** cannot be mapped by Hypo1.

program that uses a genetic algorithm to explore the full range of ligand conformational flexibility with partial flexibility of the receptor. The algorithm was tested on a data set of over 300 complexes extracted from the Brookhaven Protein DataBank.[41] GOLD succeeded in more than 70% of cases in reproducing the experimental bound conformation of the ligand.[42–44] GOLD requires a user defined binding site. It searches for a cavity within the defined area and considers all the solvent accessible atoms in the defined area as active site atoms. A 20 Å radius active site was defined considering the carboxylate oxygen (OD1) atom of residue D64 as the center of the active site. All the compounds retrieved by the pharmacophore model (Hypo 1) were docked into the active site of IN. On the basis of the GOLD fitness score, for each molecule a bound conformation with a high fitness score was considered as the best bound-conformation. All docking runs were carried out using standard default settings with a population size of 100, a maximum number of 100 000 operations, and a mutation and crossover rate of 95. The fitness function that was implemented in GOLD consisted basically of H-bonding, complex energy, and ligand internal energy terms.

Materials, Chemicals, and Enzymes. All compounds were dissolved in DMSO, and the stock solutions were stored at −20 °C. The γ [^{32}P]-ATP was purchased from either Amersham Biosciences or ICN. The expression system for the wild-type IN was a generous gift of Dr. Robert Craigie, Laboratory of Molecular Biology, NIDDK, NIH, Bethesda, MD.

Preparation of Oligonucleotide Substrates. The oligonucleotides 21top, 5′-GTGTGGAAAATCTCTAGCAGT-3′, and 21bot, 5′-ACTGCTAGAGATTTTCCACAC-3′, were purchased from Norris Cancer Center Core Facility (University of Southern California) and purified by UV shadowing on polyacrylamide gel. To analyze the extent of 3′-processing and strand transfer using 5′-end labeled substrates, 21top was 5′-end labeled using T_4 polynucleotide kinase (Epicenter, Madison, Wisconsin) and γ [^{32}P]-ATP (Amersham Biosciences or ICN). The kinase was heat-inactivated, and 21bot was added in 1.5 M excess. The mixture was heated at 95 °C, allowed to cool slowly to room temperature, and ran through a spin 25 mini-column (USA Scientific) to separate annealed double-stranded oligonucleotide from unincorporated material.

Integrase Assays. To determine the extent of 3′-processing and strand transfer, wild-type IN was preincubated at a final concentration of 200 nM with the inhibitor in reaction buffer (50 mM NaCl, 1 mM HEPES, pH 7.5, 50 μM EDTA, 50 μM dithiothreitol, 10% glycerol (w/v), 7.5 mM $MnCl_2$, 0.1 mg/ml bovine serum albumin, 10 mM 2-mercaptoethanol, 10% dimethyl sulfoxide, and 25 mM MOPS, pH 7.2) at 30 °C for 30 min. Then, 20 nM of the 5′-end ^{32}P-labeled linear oligonucleotide substrate was added, and incubation was continued for an additional 1 h. Reactions were quenched by the addition of an equal volume (16 μL) of loading dye (98% deionized formamide, 10 mM EDTA, 0.025% xylene cyanol, and 0.025% bromophenol blue). An aliquot (5 μL) was electrophoresed on a denaturing 20% polyacrylamide gel (0.09 M tris-borate pH 8.3, 2 mM EDTA, 20% acrylamide, 8 M urea).

Gels were dried, exposed in a PhosphorImager cassette, analyzed using a Typhoon 8610 Variable Mode imager (Amersham Biosciences), and quantitated using ImageQuant 5.2. Percent inhibition (*% I*) was calculated using the following equation:

$$\% I = 100[1 - (D - C)/(N - C)]$$

where *C*, *N*, and *D* are the fractions of 21-mer substrate converted to 19-mer (3′- processing product) or strand transfer products for DNA alone, DNA plus IN, and IN plus drug, respectively. The IC_{50} values were determined by plotting the logarithm of drug concentration versus percent inhibition to obtain the concentration that produced 50% inhibition.

Cells in Virus Strain. MT-4 cells were grown in a humidified atmosphere with 5% CO_2 at 37 °C and maintained in RPMI 1640 medium supplemented with 10% heat-inactivated fetal calf serum, 2 mM L-glutamine, 0.1% sodium bicarbonate, and 20 μg/mL of gentamycin.[45] The origin of HIV-1(III_B) has been described.[46]

Drug Susceptibility and Cytotoxicity Assay. Both the inhibitory effect of antiviral drugs on the HIV-induced CPE in MT-4 cell culture and compound cytotoxicity in NIH3T3 cells was determined by the MTT-assay.[47,48] This assay is based on the reduction of the yellow colored 3-(4,5-dimethylthiazol-2-yl)-2,5-diphenyltetrazolium bromide (MTT) by mitochondrial dehydrogenase of metabolically active cells to a blue formazan derivative, which can be measured spectrophotometrically. The 50% cell culture infective dose ($CCID_{50}$) of the HIV strains was determined by titration of the virus stock using MT-4 cells. For the drug-susceptibility assays, MT-4 cells were infected with 100–300 $CCID_{50}$ of the HIV strains in the presence of 5-fold serial dilutions of the antiviral drugs. The concentration of the compound achieving 50% protection against the CPE of HIV, which is defined as the IC_{50}, was determined. Cytotoxicity of the compounds was determined by measuring the viability of mock-infected MT-4 cells after 5 days of incubation.

Acknowledgment. This work was supported by funds from the Campbell Foundation to N.N.

Supporting Information Available: Chemical structures of all the inactive compounds (**29**–**73**) are provided in Table S1. This material is available free of charge via the Internet at http://pubs.acs.org.

References

(1) Dieleman, J. P.; Jambroes, M.; Gyssens, I. C.; Sturkenboom, M. C.; Stricker, B. H.; Mulder, W. M.; de Wolf, F.; Weverling, G. J.; Lange, J. M.; Reiss, P.; Brinkman, K. Determinants of recurrent toxicity-driven switches of highly active antiretroviral therapy. The ATHENA cohort. *AIDS* **2002**, *16* (5), 737–45.

(2) Potter, S. J.; Dwyer, D. E.; Saksena, N. K. Differential cellular distribution of HIV-1 drug resistance in vivo: evidence for infection of CD8+ T cells during HAART. *Virology* **2003**, *305* (2), 339–52.

(3) Yusa, K.; Harada, S. Acquisition of multi-PI (protease inhibitor) resistance in HIV-1 in vivo and in vitro. *Curr. Pharm. Des.* **2004**, *10* (32), 4055–64.

(4) Fontas, E.; van Leth, F.; Sabin, C. A.; Friis-Moller, N.; Rickenbach, M.; d'Arminio Monforte, A.; Kirk, O.; Dupon, M.; Morfeldt, L.; Mateu, S.; Petoumenos, K.; El-Sadr, W.; de Wit, S.; Lundgren, J. D.; Pradier, C.; Reiss, P. Lipid profiles in HIV-infected patients receiving combination antiretroviral therapy: are different antiretroviral drugs associated with different lipid profiles. *J. Infect. Dis.* **2004**, *189* (6), 1056–74.

(5) de Bethune, M. P.; Hertogs, K. Screening and selecting for optimized antiretroviral drugs: rising to the challenge of drug resistance. *Curr. Med. Res. Opin.* **2006**, *22* (12), 2603–12.

(6) Machouf, N.; Thomas, R.; Nguyen, V. K.; Trottier, B.; Boulassel, M. R.; Wainberg, M. A.; Routy, J. P. Effects of drug resistance on viral load in patients failing antiretroviral therapy. *J. Med. Virol.* **2006**, *78* (5), 608–13.

(7) Potter, S. J.; Lemey, P.; Dyer, W. B.; Sullivan, J. S.; Chew, C. B.; Vandamme, A. M.; Dwyer, D. E.; Saksena, N. K. Genetic analyses reveal structured HIV-1 populations in serially sampled T lymphocytes of patients receiving HAART. *Virology* **2006**, *348* (1), 35–46.

(8) Tozzi, V.; Zaccarelli, M.; Bonfigli, S.; Lorenzini, P.; Liuzzi, G.; Trotta, M. P.; Forbici, F.; Gori, C.; Bertoli, A.; Bellagamba, R.; Narciso, P.; Perno, C. F.; Antinori, A. Drug-class-wide resistance to antiretrovirals in HIV-infected patients failing therapy: prevalence, risk factors and virological outcome. *Antiviral Ther.* **2006**, *11* (5), 553–60.

(9) Cozzi-Lepri, A.; Phillips, A. N.; Ruiz, L.; Clotet, B.; Loveday, C.; Kjaer, J.; Mens, H.; Clumeck, N.; Viksna, L.; Antunes, F.; Machala, L.; Lundgren, J. D. Evolution of drug resistance in HIV-infected patients remaining on a virologically failing combination antiretroviral therapy regimen. *AIDS* **2007**, *21* (6), 721–32.

(10) Friis-Moller, N.; Reiss, P.; Sabin, C. A.; Weber, R.; Monforte, A.; El-Sadr, W.; Thiebaut, R.; De Wit, S.; Kirk, O.; Fontas, E.; Law, M. G.; Phillips, A.; Lundgren, J. D. Class of antiretroviral drugs and the risk of myocardial infarction. *N. Engl. J. Med.* **2007**, *356* (17), 1723–35.

(11) Fatkenheuer, G.; Pozniak, A. L.; Johnson, M. A.; Plettenberg, A.; Staszewski, S.; Hoepelman, A. I.; Saag, M. S.; Goebel, F. D.; Rockstroh, J. K.; Dezube, B. J.; Jenkins, T. M.; Medhurst, C.; Sullivan, J. F.; Ridgway, C.; Abel, S.; James, I. T.; Youle, M.; van der Ryst, E. Efficacy of short-term monotherapy with maraviroc, a new CCR5 antagonist, in patients infected with HIV-1. *Nat. Med.* **2005**, *11* (11), 1170–2.

(12) Nelson, M.; Fätkenheuer, G.; Konourina, I.; Lazzarin, A.; Clumeck, N.; Horban, A.; Tawadrous, M.; Sullivan, J. H.; Mayer, H.; van der Ryst, E. *Efficacy and Safety of Maraviroc Plus Optimized Background Therapy in Viremic, ART-Experienced Patients Infected with CCR5-Tropic HIV-1 in Europe, Australia, and North America: 24-Week Results.*; 14th Conference on Retroviruses and Opportunistic Infections, Los Angeles, February 25–28, 2007; Los Angeles, CA, 2007.

(13) Opar, A. New HIV drug classes on the horizon. *Nat. Rev. Drug Discovery* **2007**, *6* (4), 258–9.

(14) Dayam, R.; Al-Mawsawi, L. Q.; Neamati, N. HIV-1 Integrase inhibitors: An emerging clinical reality. *Drugs R&D* **2007**, *8* (3), 155–68.

(15) Bushman, F. D.; Craigie, R. Activities of human immunodeficiency virus (HIV) integration protein in vitro: specific cleavage and integration of HIV DNA. *Proc. Natl. Acad. Sci. U. S. A.* **1991**, *88* (4), 1339–43.

(16) Brown, P. O. Integration. In *Retroviruses*; Coffin, J. M., Hughes, S. H., Varmus, H. E., Eds.; Cold Spring Harbor Laboratory Press: Cold Spring Harbor, NY, 1997; pp 161–203.

(17) Neamati, N. Patented small molecule inhibitors of HIV-1 integrase: a 10-year saga. *Expert Opin. Ther. Pat.* **2002**, *12* (5), 709–724.

(18) Dayam, R.; Neamati, N. Small-molecule HIV-1 integrase inhibitors: the 2001–2002 update. *Curr. Pharm. Des.* **2003**, *9* (22), 1789–802.

(19) Dayam, R.; Deng, J.; Neamati, N. HIV-1 integrase inhibitors: 2003–2004 update. *Med. Res. Rev.* **2006**, *26* (3), 271–309.

(20) Pommier, Y.; Johnson, A. A.; Marchand, C. Integrase inhibitors to treat HIV/AIDS. *Nat Rev Drug Discovery* **2005**, *4* (3), 236–48.

(21) Savarino, A. A historical sketch of the discovery and development of HIV-1 integrase inhibitors. *Expert Opin Invest. Drugs* **2006**, *15* (12), 1507–22.

(22) Hazuda, D. J.; Felock, P.; Witmer, M.; Wolfe, A.; Stillmock, K.; Grobler, J. A.; Espeseth, A.; Gabryelski, L.; Schleif, W.; Blau, C.; Miller, M. D. Inhibitors of strand transfer that prevent integration and inhibit HIV-1 replication in cells. *Science* **2000**, *287* (5453), 646–50.

(23) Billich, A. S-1360 Shionogi-GlaxoSmithKline. *Curr. Opin. Invest. Drugs* **2003**, *4* (2), 206–9.

(24) Rosemond, M. J.; St. John-Williams, L.; Yamaguchi, T.; Fujishita, T.; Walsh, J. S. Enzymology of a carbonyl reduction clearance pathway for the HIV integrase inhibitor, S-1360: role of human liver cytosolic aldo-keto reductases. *Chem. Biol. Interact.* **2004**, *147* (2), 129–39.

(25) Deng, J.; Dayam, R.; Al-Mawsawi, L. Q.; Neamati, N. Design of second generation HIV-1 integrase inhibitors. *Curr. Pharm. Des.* **2007**, *13* (2), 129–41.

(26) Markowitz, M.; Morales-Ramirez, J. O.; Nguyen, B. Y.; Kovacs, C. M.; Steigbigel, R. T.; Cooper, D. A.; Liporace, R.; Schwartz, R.; Isaacs, R.; Gilde, L. R.; Wenning, L.; Zhao, J.; Teppler, H. Antiretroviral activity, pharmacokinetics, and tolerability of MK-0518, a novel inhibitor of HIV-1 integrase, dosed as monotherapy for 10 days in treatment-naive HIV-1-infected individuals. *J. Acquired Immune Defic. Syndr.* **2006**, *43* (5), 509–15.

(27) Grinsztejn, B.; Nguyen, B. Y.; Katlama, C.; Gatell, J. M.; Lazzarin, A.; Vittecoq, D.; Gonzalez, C. J.; Chen, J.; Harvey, C. M.; Isaacs, R. D. Safety and efficacy of the HIV-1 integrase inhibitor raltegravir (MK-0518) in treatment-experienced patients with multidrug-resistant virus: a phase II randomised controlled trial. *Lancet* **2007**, *369* (9569), 1261–9.

(28) Cooper, D.; Gatell, J.; Rockstroh, J.; Katlama, C.; Yeni, P.; Lazzarin, A.; Chen, J.; Isaacs, R.; Teppler, H.; Nguyen, B.; and for the BENCHMRK-Study Group. *Results of BENCHMRK-1, a Phase III Study Evaluating the Efficacy and Safety of MK-0518, a Novel HIV-1 Integrase Inhibitor, in Patients with Triple-Class Resistant Virus*; 14th Conference on Retroviruses and Opportunistic Infections, Los Angeles, USA, February 25–28, 2007; Los Angeles, CA, 2007.

(29) Steigbigel, R.; Kumar, P.; Eron, J.; Schechter, M.; Markowitz, M.; Loufty, M.; Zhao, J.; Isaacs, R.; Nguyen, B.; Teppler, H.; and for the BENCHMRK-Study Group. *Results of BENCHMRK-2, a Phase III Study Evaluating the Efficacy and Safety of MK-0518, a Novel HIV-1 Integrase Inhibitor, in Patients with Triple-Class Resistant Virus*; 14th Conference on Retroviruses and Opportunistic Infections, Los Angeles, USA, February 25–28, 2007; Los Angeles, CA, 2007.

(30) Sato, M.; Motomura, T.; Aramaki, H.; Matsuda, T.; Yamashita, M.; Ito, Y.; Kawakami, H.; Matsuzaki, Y.; Watanabe, W.; Yamataka, K.; Ikeda, S.; Kodama, E.; Matsuoka, M.; Shinkai, H. Novel HIV-1 integrase inhibitors derived from quinolone antibiotics. *J. Med. Chem.* **2006**, *49* (5), 1506–8.

(31) DeJesus, E.; Berger, D.; Markowitz, M.; Cohen, C.; Hawkins, T.; Ruane, P.; Elion, R.; Farthing, C.; Zhong, L.; Cheng, A. K.; McColl, D.; Kearney, B. P. Antiviral activity, pharmacokinetics, and dose response of the HIV-1 integrase inhibitor GS-9137 (JTK-303) in treatment-naive and treatment-experienced patients. *J. Acquired Immune Defic. Syndr.* **2006**, *43* (1), 1–5.

(32) Zolopa, A. R.; Mullen, M.; Berger, D.; Ruane, P.; Hawkins, T.; Zhong, L.; Chuck, S.; Enejosa, J.; Kearney, B.; Cheng, A. *The HIV Integrase Inhibitor GS-9137 Demonstrates Potent Antiretroviral Activity in Treatment-Experienced Patients*; 14th Conference on Retroviruses and Opportunistic Infections, Los Angeles, USA., February 25–28, 2007; Los Angeles, CA, 2007.

(33) Jones, G.; Ledford, R.; Yu, F.; Miller, M.; Tsiang, M.; McColl, D. *Resistance Profile of HIV-1 Mutants in Vitro Selected by the HIV-1 Integrase Inhibitor, GS-9137 (JTK-303)*; 14th Conference on Retroviruses and Opportunistic Infections, Los Angeles, February 25–28, 2007; Los Angeles, CA, 2007.

(34) Catalyst; Accelrys, Inc.: San Diego, CA.

(35) Smellie, A.; Dyda, F.; Hickman, A. B. Poling-Promoting conformational variation. *J. Comput. Chem.* **1995**, *16*, 171–187.

(36) Smellie, A.; Kahn, S. D.; Teig, S. L. Analysis of conformational coverage 0.1. Validation and estimation of coverage. *J. Chem. Inf. Comput. Sci.* **1995**, *35* (2), 285–294.

(37) Smellie, A.; Kahn, S. D.; Teig, S. L. Analysis of conformational coverage 0.2. Application of conformational models. *J. Chem. Inf. Comput. Sci.* **1995**, *35* (2), 295–304.

(38) Goldgur, Y.; Dyda, F.; Hickman, A. B.; Jenkins, T. M.; Craigie, R.; Davies, D. R. Three new structures of the core domain of HIV-1 integrase: an active site that binds magnesium. *Proc. Natl. Acad. Sci. U. S. A.* **1998**, *95* (16), 9150–4.

(39) Goldgur, Y.; Craigie, R.; Cohen, G. H.; Fujiwara, T.; Yoshinaga, T.; Fujishita, T.; Sugimoto, H.; Endo, T.; Murai, H.; Davies, D. R. Structure of the HIV-1 integrase catalytic domain complexed with an inhibitor: a platform for antiviral drug design. *Proc. Natl. Acad. Sci. U. S. A.* **1999**, *96* (23), 13040–3.

(40) GOLD 3.1; The Cambridge Crystallographic Data Centre: Cambridge, U.K., 2005.

(41) Berman, H. M.; Westbrook, J.; Feng, Z.; Gilliland, G.; Bhat, T. N.; Weissig, H.; Shindyalov, I. N.; Bourne, P. E. The Protein Data Bank. *Nucleic Acids Res.* **2000**, *28* (1), 235–42.

(42) Nissink, J. W.; Murray, C.; Hartshorn, M.; Verdonk, M. L.; Cole, J. C.; Taylor, R. A new test set for validating predictions of protein-ligand interaction. *Proteins* **2002**, *49* (4), 457–71.

(43) Verdonk, M. L.; Cole, J. C.; Hartshorn, M. J.; Murray, C. W.; Taylor, R. D. Improved protein-ligand docking using GOLD. *Proteins* **2003**, *52* (4), 609–23.

(44) Verdonk, M. L.; Chessari, G.; Cole, J. C.; Hartshorn, M. J.; Murray, C. W.; Nissink, J. W.; Taylor, R. D.; Taylor, R. Modeling water molecules in protein-ligand docking using GOLD. *J. Med. Chem.* **2005**, *48* (20), 6504–15.

(45) Miyoshi, L.; Taguchi, H.; Kobonishi, I.; Yoshimoto, S.; Ohtsuki, Y.; Shiraishi, Y. Type C virus-producing cell lines derived from adult T cell leukemia. *Gann Monogr. Cancer Res.* **1982**, *28*, 219–28.

(46) Popovic, M.; Sarngadharan, M. G.; Read, E.; Gallo, R. C. Detection, isolation, and continuous production of cytopathic retroviruses (HTLV-III) from patients with AIDS and pre-AIDS. *Science* **1984**, *224* (4648), 497–500.

(47) Pauwels, R.; Balzarini, J.; Baba, M.; Snoeck, R.; Schols, D.; Herdewijn, P.; Desmyter, J.; De Clercq, E. Rapid and automated tetrazolium-based colorimetric assay for the detection of anti-HIV compounds. *J. Virol. Methods* **1988**, *20* (4), 309–21.

(48) Witvrouw, M.; Pannecouque, C.; Switzer, W. M.; Folks, T. M.; De Clercq, E.; Heneine, W. Susceptibility of HIV-2, SIV and SHIV to various anti-HIV-1 compounds: implications for treatment and post-texposure prophylaxis. *Antiviral Ther.* **2004**, *9* (1), 57–65.

JM070609B